

An energy absorption system based on carbon nanotubes and nonaqueous liquid

Weiyi Lu, Venkata K. Punyamurtula, Yu Qiao

*Department of Structural Engineering, University of California – San Diego, La Jolla, CA
92093-0085, USA*

By forcing paraxylene into single wall carbon nanotubes, a large amount of external work can be converted to excess solid-liquid interfacial energy. Due to the hysteresis of sorption isotherm curves, as the external pressure is decreased, only a small fraction of the interfacial energy can be released, making this system attractive for design of advanced energy absorption devices. As the infiltration-defiltration loop continues, the energy absorption process can be repeated at a reduced level.

Keywords: Nanotubes; Infiltration; Energy absorption

1. Introduction

Carbon nanotubes (CNTs) have been studied extensively for the past decade [1]. The CNTs are of excellent mechanical, electrical, and thermal properties, providing promising ways for the development of advanced nanocomposites, energy related nanodevices, nanosensors, nanotransportation techniques, etc. [2–4]. Currently, most of the studies in this area are focused on the CNT networks and their interactions with external environments, compared with which the utility of the large inner wall area is relatively un-investigated.

Using the empty space in a porous media for selective absorption, catalysis, etc. has long been an active area of research [5]. Recently, with the progress in processing techniques of nanoporous materials, their application has been extended to energy absorption structures [6–11], for protection layers, damping stages, blast-mitigating columns, etc. Nanoporous materials are solids containing large volume fractions of pores that are of the diameters in the range of 0.5 nm to 1000 nm. With a given pore volume fraction, the smaller the pore size, the larger the specific surface area would be. For the materials of pore sizes smaller than 2 nm, which are often referred to as microporous materials, the specific surface areas are typically around $1000 \text{ m}^2\text{g}^{-1}$. For mesoporous materials, where pore sizes are smaller than 50 nm but larger than 2 nm, the specific surface areas are $100\text{--}300 \text{ m}^2\text{g}^{-1}$. As the large surface area is exposed to a nonwetting liquid, for example by forcing the liquid into the nanopores under a sufficiently high external pressure, the system free energy can be increased significantly, at the level of $10\text{--}100 \text{ Jg}^{-1}$ [12]. That is, a large portion of the work done by the external pressure is transformed to the solid–liquid interfacial energy. The sorption isotherms of many nanoporous materials exhibit hysteretic characteristics. As the external pressure is decreased, the unloading path can be considerably different from the loading path; i.e. the defiltration pressure can be much lower than the infiltration pressure. Consequently, only a small portion of the excess solid–liquid interfacial energy can be released, and the rest part should be regarded as being dissipated or being “absorbed”, which, compared with the energy absorption efficiency of conventional damping materials [13], is larger by 1–2 orders of magnitude.

It is envisioned that a similar technique can be applied to CNTs. Here, the most attractive feature of the CNT is its high specific area of inner wall surface. As it is forced to expose to a nonwetting liquid, the mechanical work to interfacial energy transition can take place. If this process is irreversible, the system becomes energy absorbing. A proof-of-concept study has been carried out by using a multiwall CNT [14]. In the current study, we investigate a single-wall CNT (SWCNT) that is of a larger specific surface area, so as to further increase the energy absorption efficiency.

2. Experimental

The experimental setup was formed by sealing 0.15 g of Aldrich 589705 SWCNT with a liquid phase in a steel cylinder, using a piston with a reinforced gasket. The average diameter was about 1 nm, with the standard deviation of about 0.3 nm. The CNT lengths were in the range of 2 to 20 μm . They formed bundles of about 20 CNTs, with impurities of carbon-coated metal nanoparticles and amorphous phases. The impurities were solid particles, and therefore should not affect the liquid infiltration process. The density of the CNT was 1.8 g/ml at room temperature.

The inner surface of the CNT under investigation was effectively hydrophilic; that is, when it was immersed in water, infiltration could take place spontaneously even without any external pressure. Thus, the liquid phase in the infiltration experiment was chosen as the nonpolar paraxylene (C_8H_{10}), which is an aromatic hydrocarbon, with two methyl substituents in a benzene ring. Its molecular weight is 106.2, and the molecular size is about 0.5 nm, smaller than the size of the CNT. By using an Instron machine, the piston was compressed into the steel cylinder at a constant rate of $0.5 \text{ mm}\cdot\text{min}^{-1}$. The friction between the piston and the cylinder was less than 0.5 % of the peak load. The force acting on the piston, F , was measured by a 50KN loadcell and the piston displacement, d , was recorded by a linear variable displacement transducer. The pressure in the liquid phase was calculated as F/A , and the system volume decrease was calculated as $d\cdot A$, with $A = 287 \text{ mm}^2$ being the cross-sectional area of the steel cylinder. After the pressure reached 150 MPa, the piston was moved out of the cylinder at the same rate, leading to the unloading of the liquid phase, until the piston returned to its original position and a complete loading–unloading cycle was finished. Such cycles were repeated 6 times and altogether three nominally identical samples were tested. The time interval between two loading cycles, i.e. the time from the end of unloading of the previous cycle to the beginning of loading of the next cycle, was about 30 sec. Figure 1 shows a typical set of sorption isotherm curves. Note that in order to compare the system volume variation the curves have been shifted along the horizontal axis, so that the onset of linear compression section starts from the origin.

3. Results and discussion

The widest loop in Fig. 1 indicates the sorption isotherm curve of the CNT based system at the first loading. The specific system volume change is defined as $d\cdot A/m$, where $m = 0.15 \text{ g}$ is the mass of the CNT. Initially, the pressure is relatively low and insufficient to overcome the capillary effect. Thus, since the CNT is lyophobic, the paraxylene molecules cannot enter the inner space of them. When the pressure reaches 23 MPa, it becomes more energetically favorable for the liquid to infiltrate into the largest CNTs, as depicted in Fig. 2. Under this condition, the

release of hydrostatic pressure can be balanced by the increase in solid-liquid interfacial energy. That is,

$$P^2/2K(\pi r^2 l) = \Delta\gamma 2\pi r \quad (1)$$

which can be rewritten as

$$\Delta\gamma = P^2 r / 4K \quad (2)$$

where $\Delta\gamma$ is the excess solid-liquid interfacial tension, P is the external pressure, K is the effective bulk modulus of the liquid phase, r is the CNT radius, and l is the effective infiltration depth of liquid molecules. If r is taken as 0.6 nm and K is set as 2 GPa, $\Delta\gamma$ can be assessed as $0.04 \text{ mJ}\cdot\text{m}^{-2}$, which is quite small compared with that of silica based systems [15], indicating that the relatively large value of infiltration pressure should be attributed to the small CNT diameter. Note that immediately after the infiltration begins, there is a relatively small decrease in pressure, which is consistent with the fact that to enter a CNT a liquid molecule must be partly isolated from the surrounding liquid molecules by carbon atoms, while when it moves deeper into the CNT no new solid-liquid interactions need to be established. Therefore, the energy barrier for the liquid to begin to infiltrate into a CNT is larger than that of the continuous infiltration. In the above discussion, the effects of CNT deformation and the associated thermal effects are ignored, as the CNTs are much more rigid than the liquid phase, especially during the infiltration process.

For the CNT under investigation, the diameter exhibits a distribution, i.e. different CNTs may be of different diameters, which scatter in a relatively broad range. The diameter of the thinnest CNT can be a few times smaller than that of the largest ones. Consequently, as more and more CNTs are involved in the pressure induced infiltration, the external pressure must be increasingly high, leading to the finite slope of the infiltration plateau of the sorption isotherm. When the pressure is increased to 150 MPa, most of the empty space of CNT is filled and the slope of sorption isotherm is much larger than that at the beginning section of the infiltration plateau, close to that in the initial linear compression stage.

When the external pressure is lowered, the unloading path is significantly different from the loading path. The confined liquid in the CNT does not defiltrate immediately when P is smaller than the infiltration pressure, suggesting that liquid infiltration and defiltration are governed by different mechanisms. The infiltration, as discussed above, is a result of the competition of the release of external pressure and the increase in solid-liquid interfacial energy. The defiltration, on the other hand, should be associated with the gas phase nucleation and growth and their influences on motions of confined liquid molecules [16]. Consequently, during unloading, when the pressure is relatively high the sorption isotherm curve is quite linear. Note that the bulk modulus of the system, which can be measured by the slope of linear section of sorption isotherm curve, during unloading is quite different from that during loading, probably due to the difference in effective stiffness of an empty CNT and a filled CNT. Because of the inner pressure caused by the capillary effect, a CNT filled by the paraxylene molecules is stretched and thus its deformability under the same pressure may be smaller.

As the pressure is reduced to lower than 22 MPa, nearly the same as the pressure at the onset of infiltration, the defiltration starts. The slope of sorption isotherm curve becomes much smaller. Unlike the loading path, the defiltration part is quite linear, which, again, confirms that the defiltration mechanism is different from the infiltration mechanism. The defiltration continues until the pressure is entirely removed; however, not all the confined liquid molecules come out. Thus, the unloading path does not end at the origin. The hysteresis of sorption isotherm causes the energy absorption behavior. The energy absorption efficiency is measured by the area enclosed by the infiltration-defiltration loop, which is about 130 Jg^{-1} , much higher

than that of conventional damping materials, especially when compared with ordinary liquid-containing protection and damping systems where the incompressible liquid phases, e.g. water, can only redistribute but not absorb input energy.

As the loading–unloading cycle is repeated, similar energy absorption characteristics can be observed. However, the system volume change associated with the infiltration plateau decreases as the loading cycle continues. For self-comparison purpose, in the current study the width of infiltration plateau is defined as the distance from the end of the initial linear compression section, at which the local maximum pressure prior to the slight pressure decrease is reached, to the point of sorption isotherm curve where the slope equals 50 % of that of the linear section of unloading part. The infiltration pressure is defined as the pressure at the middle point of this area. In the first loading cycle, the infiltration volume is around $2.7 \text{ cm}^3\text{g}^{-1}$, which quickly decreases to about $0.8 \text{ cm}^3\text{g}^{-1}$ after two loading cycles, and is then stabilized at this level. Correspondingly, while the pressures at the onset of infiltration and the onset of defiltration are nearly constant, the infiltration pressure decreases monotonically as the loading cycle continues. In the first four cycles, it rapidly decreases from 55 MPa to 33 MPa. Further repeating the infiltration–defiltration process does not lead to pronounced variation in infiltration pressure. Clearly, due to the difficulty in defiltration, a part of the confined liquid remains in the CNTs even after the external pressure is removed, and therefore less empty space is available for the next infiltration cycle. The infiltrated liquid contains a reversible part and an irreversible part. The irreversible part deactivates the associated CNT space, and the reversible part makes the system usable under a cyclic loading. According to the testing data, the reversible part takes about 1/3 and the irreversible part takes about 2/3 of the total CNT space. The factors dominating the non-defiltration can be related to the irregular configurations of poorly formed CNTs, the blocking effect of impurities, and/or the energy barrier of gas phase nucleation [16], the details of which are still under investigation. Note that the width of infiltration plateau in the next cycle is slightly larger than the width of defiltration plateau of the previous one, indicating that during the resting period between two loading cycles a certain amount of confined liquid diffuses out, which is in agreement with previous experimental observations of a nanoporous silica [16].

Because both of the infiltration pressure and the infiltration volume decrease as the cyclic loading continues, the energy absorption capacity per loading cycle also decreases, as shown in Fig. 3. The peak value of energy absorption efficiency is achieved at the first loading, and after a few cycles it is reduced to about 25 Jg^{-1} , which is still much higher than that of previously developed nanoporous systems [17]. As more loading cycles are applied, further decrease in energy absorption efficiency is negligible, which should be attributed to that, after the irreversible part of the confined liquid occupies about 2/3 of the CNT inner space, the remaining part is reversible. The accumulated energy is shown as the dashed line in Fig. 3. In the first three loading cycles, the total absorbed energy is about 250 Jg^{-1} , after which the energy absorption capacity is stabilized at about 25 Jg^{-1} per cycle.

4. Concluding remarks

The energy absorption performance of a lyophobic single-wall CNT immersed in paraxylene is investigated via infiltration experiment. Associated with the pressure induced infiltration and the incomplete defiltration, a significant part of the external work is dissipated, and therefore this system can be used for protection or damping applications. The confined liquid consists of a reversible part and an irreversible part. The former makes the system energy

absorbing under a cyclic loading, and the latter leads to a high energy absorption capacity in the first a few loading cycles. The testing data show that the mechanisms of infiltration and defiltration are different.

This work was supported by The Army Research Office under Grant No. W911NF-05-1-0288.

Correspondence Address:

Dr. Yu Qiao
Department of Structural Engineering
University of California, San Diego
9500 Gilman Dr. MC 0085
La Jolla, CA 92093-0085, USA
Tel.: 858-534-3388
Fax: 858-534-1310
Email: yqiao@ucsd.edu

References

- [1] M.J. O’Connell; Carbon Nanotubes, CRC Press, 2006.
- [2] K. Tanaka, T. Yamabe, K. Fukui; The Science and Technology of Carbon Nanotubes, Elsevier Sci., 1999.
- [3] J.P. Salvetat, S. Bhattacharyya, R.B. Pipes; *J. Nanosci. Nanotech.* 6 (2006) 1857-1882.
- [4] M. Meyyappan; Carbon Nanotubes: Science and Applications, CRC Press, 2004.
- [5] J. Bear; Dynamics of Fluids in Porous Media, Dove Publ., 1988.
- [6] X. Kong, Y. Qiao; Improvement of recoverability of a nanoporous energy absorption system by using chemical admixture, *Appl. Phys. Lett.* 86 (2005) 151919.
- [7] F.B. Surani, X. Kong, D.B. Panchal, Y. Qiao; Energy absorption of a nanoporous system subjected to dynamic loadings, *Appl. Phys. Lett.* 87 (2005) 163111.
- [8] F.B. Surani, X. Kong, Y. Qiao; Two-staged sorption isotherm of a nanoporous energy absorption system, *Appl. Phys. Lett.* 87 (2005) 251906.
- [9] F.B. Surani, A. Han, Y. Qiao; An experimental investigation on pressurized liquid in confining nanoenvironment, *Appl. Phys. Lett.* 89 (2006) 093108.
- [10] A. Han, Y. Qiao; Pressure induced infiltration of aqueous solutions of multiple promoters in a nanoporous silica. *J. Am. Chem. Soc.* 128 (2006) 10348-10349.
- [11] F.B. Surani, Y. Qiao; Infiltration and defiltration of an electrolyte solution in nanopores. *J. Appl. Phys.* 100 (2006) 034311.
- [12] A. Han, V.K. Punyamurtula, T. Kim, Y. Qiao; The upper limit of energy density of nanoporous materials functionalized liquid. *J. Mater. Eng. Perf.* 17, 326-329 (2008).
- [13] G. Lu, T. Yu; Energy Absorption of Structures and Materials, CRC Press, 2003.
- [14] V.K. Punyamurtula, Y. Qiao; Hysteresis of sorption isotherm of multiwall carbon nanotube in paraxylene, *Materials Research Innovations* 11, 37-39 (2007)
- [15] X. Kong, F.B. Falgun, Y. Qiao; Energy absorption of nanoporous silica particles in aqueous solutions of sodium chloride. *Phys. Scripta* 74, 531-534 (2006)

- [16] A. Han, X. Kong, Y. Qiao; Pressure induced infiltration in nanopores. *J. Appl. Phys.* 100 (2006) 014308.
- [17] F.B. Surani, Y. Qiao; Energy absorption of a polyacrylic acid partial sodium salt modified nanoporous system. *J. Mater. Res.* 21 (2006) 1327-1330.

Figures and Figure Captions

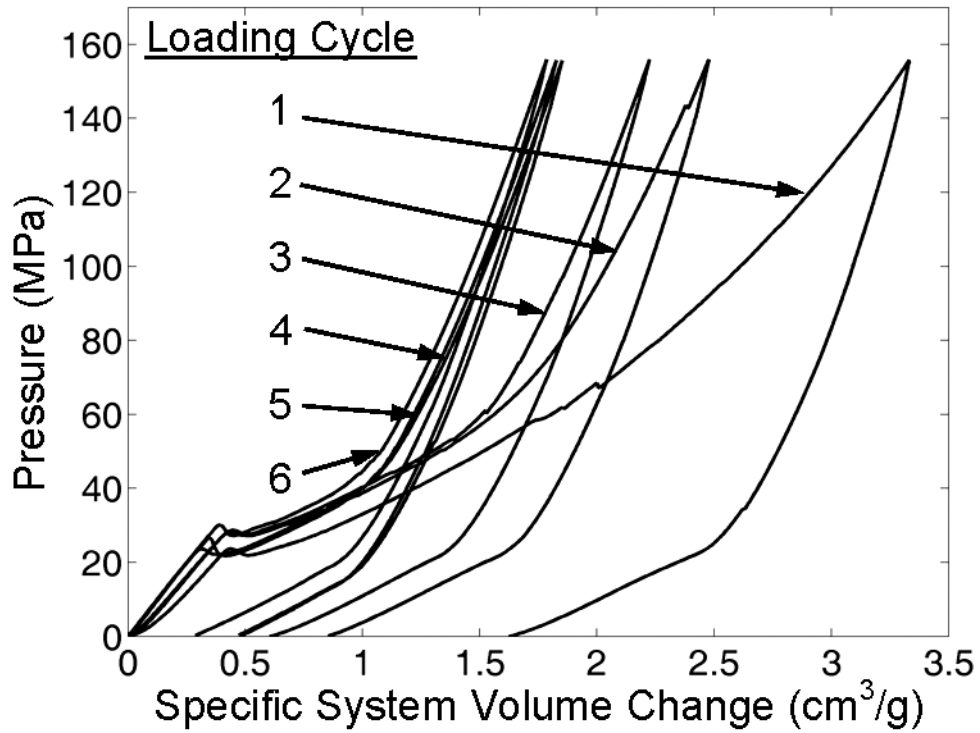


Fig.1 Typical sorption isotherm curves. The curves have been shifted along the horizontal axis.

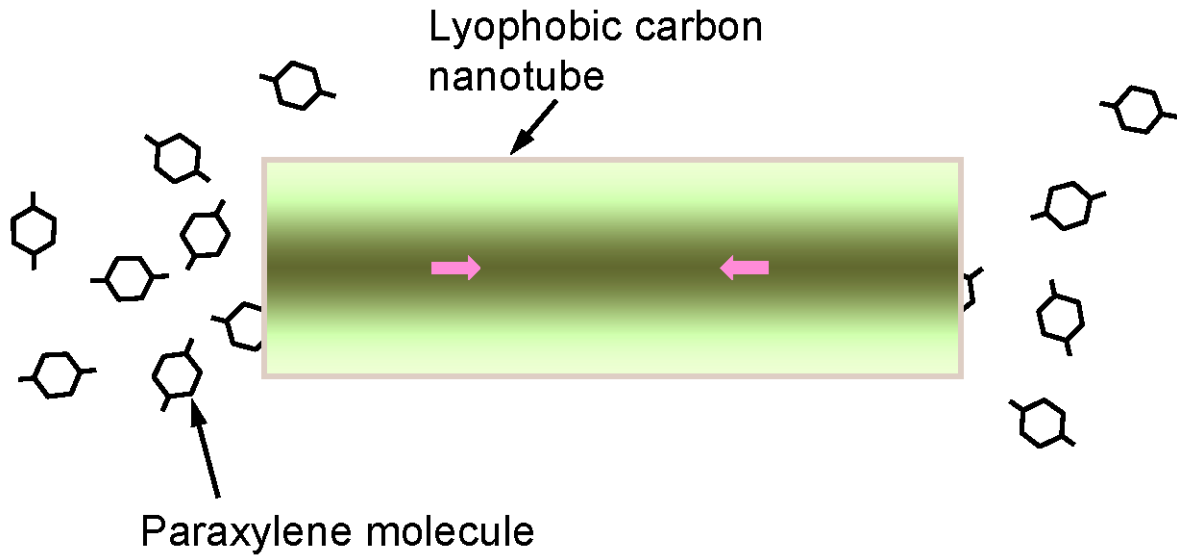


Fig.2 A schematic diagram of infiltration of paraxylene molecules in a carbon nanotube.

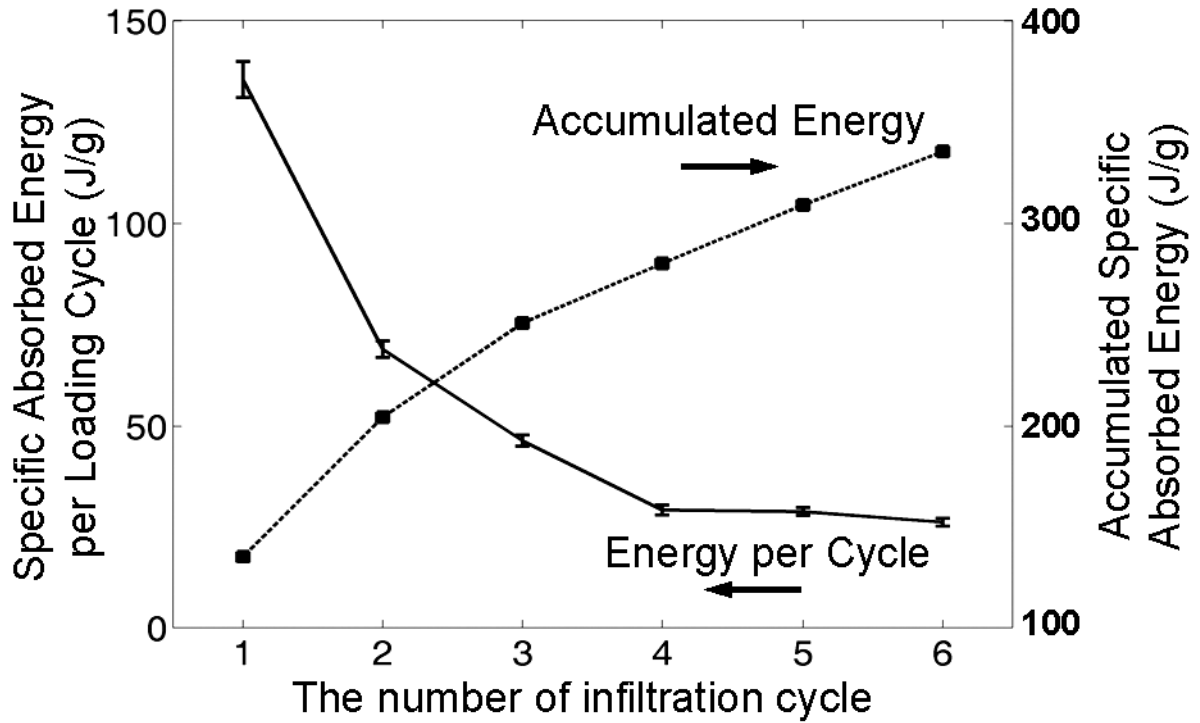


Fig.3 The change in energy absorption capacity and the accumulated energy as the infiltration-defiltration cycle continues.